# XIV Reunión del Comité de Optoelectrónica

2-4 julio 2025, Terrassa

# - LIBRO DE ACTAS -

optoel 2025

Center for Sensors, Instruments and System Development - UPC

## COMITÉ EDITORIAL





ISBN: 979-13-87613-54-9
DOI: 10.5821/ebook-9791387613549

# Towards improved performance of an Yb:KGW laser-based intracavity image upconverter

Adrián J. TORREGROSA[(1)], María Luisa RICO[(2)], Juan CAPMANY[(1)], Miguel CUENCA[(1)], Angela E. ORTEGA[(1)], Carlos R. FERNÁNDEZ-POUSA[(1)] and Haroldo MAESTRE[(1)]

1. Engineering Research Institute of Elche-I3E, Universidad Miguel Hernandez de Elche, Avda. de la Universidad s/n, 03202 Elche (Alicante), Spain.
2. Computer Science Department, Universidad de Alicante, Ctra. San Vicente s/n, 03690 San Vicente del Raspeig (Alicante), Spain

Contact: Haroldo MAESTRE (hmaestre@umh.es).

**ABSTRACT:**

This paper presents an Yb:KGW laser-based intracavity image upconverter designed to enhance mid-IR imaging. Traditional mid-IR imaging faces limitations in sensor efficiency, resolution, and cost. Our approach uses IR to visible frequency shift imaging with non-linear Sum-Frequency Mixing (SFM) processes for real-time imaging using Si-based CMOS detectors. Key improvements include the use of a CPLN crystal for increased spectral and angular acceptance, broad SFM pump beams for high spatial resolution, and q-switched intracavity conversion to boost intensity and compensate for efficiency reduction tradeoffs. Additionally, we demonstrate that asymmetric laser modes within the cavity enhance image resolution. Results show successful real-time upconversion of mid-IR images to NIR. These characteristics pave the way for future high-performance mid-IR image upconverters and applications.

**Key words:** Image upconversion, Infrared imaging, Nonlinear optics, Solid-state lasers

## 1.- Introduction

Imaging in the mid and far infrared lacks image sensor arrays with high efficiency, high resolution and number of pixels, high speed and low cost [1]. Although imaging techniques in these bands have a wide range of applications, the lack of high-performance image sensors limits their widespread use. Infrared (IR) to visible frequency shift imaging is presented as an alternative, a technique that allows real-time imaging using conventional detectors (Si-based CMOS) with mature technology and high resolution and efficiency in potentially any spectral region [2].

This optical frequency upconversion technique is mostly based on non-linear Sum Frequency Mixing (SFM) processes. In SFM processes for imaging, an intense wave around 1 μm (SFM pump) is mixed with a wave in the mid-IR and a new wave is generated with a wavelength in the near infrared (NIR) that falls within the silicon absorption band (SFM or upconverted wave). The frequency shift can be applied to complete real-time images and is typically performed using a 4f imaging system with a non-linear optical crystal in the Fourier plane [3].

The IR image, thus, enters the 4f system and, after passing through the first lens, the spatial information is transformed into frequency information in the Fourier plane. This is where the non-linear crystal is located and where the image mixes with the SFM pump. The intensity of the SFM pump determines the efficiency of the IR to NIR frequency shift and, depending on the beam size of the SFM pump, it allows the conversion (equivalent to

transmission in a conventional 4f) of more or less infrared spatial frequencies to the NIR, where the new image, after passing through the second lens, is detected by high performance sensors. As it can be inferred, there is a trade-off here between the conversion efficiency and the resolution of the upconverter. These two characteristics are inversely related, as a very narrow SFM pump mode allows high optical intensity but avoids conversion of high spatial frequencies, and vice versa. Conversely, the properties of the nonlinear crystal dictate the nonlinear coefficient and phase matching, which in turn influence conversion efficiency, the range of wavelengths that can be converted, and the angular acceptance of the input image (field-of-view). One of the most commonly used non-linear crystals is $LiNbO_3$ with a periodically polarized domain structure (PPLN) due to its ferroelectric nature. Although these crystals have high efficiency, their wavelength and angular acceptances are narrow. To enhance these parameters, $LiNbO_3$ crystals with a chirped domain structure (CPLN) can be employed to significantly boost the angular and spectral acceptances, though at the expense of efficiency [4].

The aforementioned crystals have a typical thickness of 1 mm due to the manufacturing process, which also limits the achievable SFM pump beam diameter to <1mm and so the maximum spatial resolution, particularly in intracavity upconversion. This limitation does not occur in the direction perpendicular to the thickness. In this sense, it may be advantageous to use a wide SFM pumping mode in the dimension where the crystal does not represent a size constraint, and to transfer the improved resolution to the two spatial directions by rotating the sample and with targeted reconstruction software. This has been recently demonstrated in an external cavity configuration [5].

In this work, we combine a number of techniques to create an image converter by optimizing the key parameters of these systems in a single device, as outlines below:

1- Use of a CPLN crystal to increase the spectral (hyperspectral capability) and angular (field-of-view) acceptance of the converter.
2- Broad beam size of the SFM pump for high spatial resolution.
3- Q-switched intracavity conversion to boost the intensity of SFM pump and to compensate for the efficiency reduction due to the use of a broad beam.
4- The implementation of an asymmetrical SFM pumping mode is intended to address the limitations imposed by size constraints.

## 2.- Experimental setup of the upconverter

We present in Fig. 1 the experimental implementation of the intracavity image upconverter. The setting comprises a four mirror z-folded laser cavity. All mirrors (M1, M2, M3 and M4) are flat mirrors with highly reflective (HR) coatings at 1040 nm. In addition, M1 is antireflection (AR) coated at 981 nm and M4 is AR coated at 4 µm, respectively. The laser cavity has a total length (M1 to M4) of 150 mm. Since all cavity mirrors are flat, a 100 mm intracavity lens (ICL) is inserted to make the cavity stable. When ICL is around one focal length from M1 it provides an intracavity laser mode which focuses to a waist of 50 µm radius near M1, and becomes a collimated beam between ICL and M4 with a radius of ~500 µm. This configuration is adequate for good laser efficiency in the Yb:KGW crystal and good resolution in the non-linear crystal.

The laser crystal is placed near M1 and is a 3 mm x 3 mm cross sectional area, 4 mm long, $N_g$-cut Yb:KGW doped 3% at., which generates laser emission around 1040 nm in $N_p$-polarization. The Yb:KGW is pumped with a fiber-coupled (NA=0.22, 105 µm core) 981 nm laser diode (LD). The Yb:KGW laser can be operated in either CW or passively qswitched regimes. For passively q-switched operation, a Cr:YAG saturable absorber (SA), AR coated at 1040 nm and with an initial transmission $T_0$=90%, is inserted near M2. The non-linear crystal, where the upconversion takes place, is placed in the M3-M4 cavity arm. The nonlinear crystal is a CPLN crystal for broadband mid-IR

upconversion with a wide field-of-view and it is AR coated at the wavelengths of interest. The CPLN crystal is, simultaneously, placed at the Fourier plane of a 4f-system, with L1 and L2 imaging lenses. The CPLN has a linearly chirped poling period ranging from 19-24 μm, which means that mid-IR wavelengths from 2-4.5 μm can be phase-matched and upconverted with a field-of-view as wide as 30º.

The 4 μm radiation from a quantum-cascade laser (QCL) is collimated, transmitted through an USAF 1951 target for image formation and focused into the CPLN by means of L1. The mid-IR image and the intracavity SFM pump are mixed in the CPLN, taking advantage of the high intracavity 1040 nm intensity (CW or pulsed), which results in a high frequency conversion efficiency. Consequently, the mid-IR image is shifted to a new image of 825 nm which can be detected with a silicon CCD/CMOS high-sensitivity and high-resolution camera after propagation through L2.

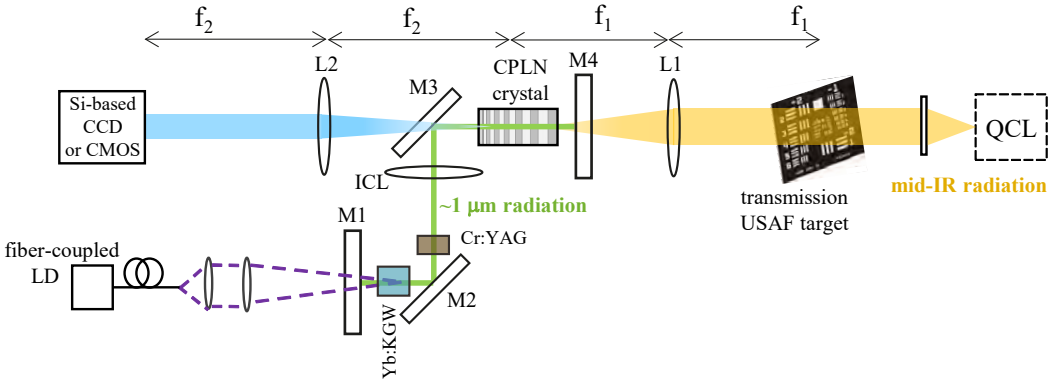


*Fig. 1: Experimental setting of the proposed mid-IR image upconverter.*

## 3.- Experimental results

Preliminary data on the converter characteristics are presented below. This section focuses on showing the conversion of mid-IR images to NIR, the intracavity q-switched operation to achieve high conversion efficiencies and the improvement of the converted image resolution by using asymmetric laser modes within the cavity.

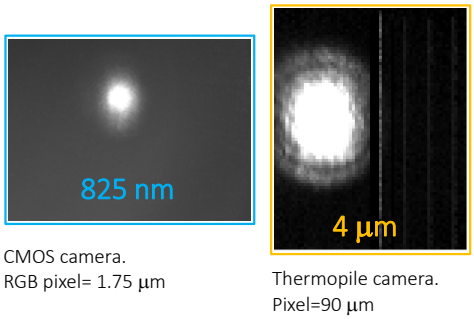


*Fig. 2: Upconversion of the QCL laser transverse profile from mid-IR to the NIR.*

### 3.1.- Intracavity mid-IR image upconversion

The intracavity power at 1040 nm in the Yb:KGW laser allows the image to be shifted from 4 μm to 825 nm and by SFG in the CPLN and detected by the Si camera. This conversion takes place in real time (as many frames/s as the CCD/CMOS camera allows) and, by operating in the Fourier plane of the 4f system, all the pixels are converted simultaneously without the need for spatial scanning techniques (raster scanning, etc...).

For comparison, the QCL laser mode image obtained directly on a pyroelectric array sensor and the NIR converted image detected with a Si-based CMOS camera are presented (Fig. 2). The frame colour of the images corresponds to the colours of the different optical bands depicted in Fig. 1. Despite the conversion being associated with a reduction in image size of the order of ρ, this factor can be compensated by the magnification of $\frac{\lambda_{up}}{\lambda_{IR}} \sim 5$ of the 4f system. Fig. 3 demonstrates the conversion of a USAF 1951 image (group

1, elements 5 and 6) from 4 µm to 825 nm and its visualization on a CMOS camera, as well as the magnification of the conversion by varying the ratio of f1 to f2 of the 4f system.

The portrayed uconversions were performed in CW regime and the conversion was appreciable from the moment the QCL laser emission threshold was reached. Alternatively, in CW, for a pump diode power at 981 nm absorbed of 5 W, approximately 60 W of intracavity power is achieved at 1040 nm.

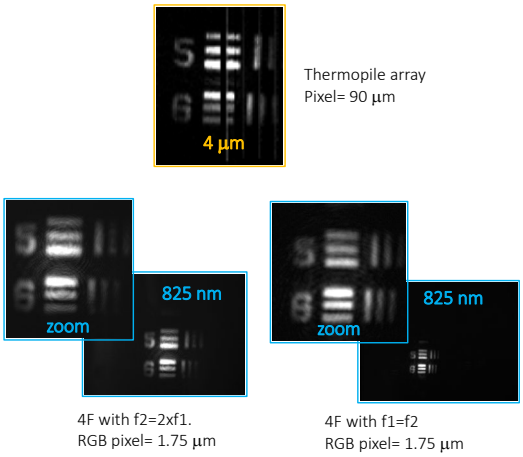


*Fig. 3: Upconversion of mid-IR USAF 1951 images (group 1, elements 5 and 6) wavelength shifted to 825 nm for different remagnification ratios of the 4f system.*

### 3.2.- Intracavity q-switched operation

In addition to continuous wave operation, the converter can be used in q-switched mode by inserting a Cr:YAG SA in the laser cavity. This configuration enables the attainment of pulsed emission within the pumping cavity of the SFM, with peak powers that reach of 100 kW, pulses with durations ranging from 20 to 30 ns, and repetition frequencies spanning from 8 to 20 kHz.

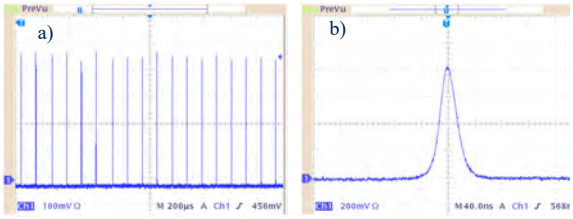


*Fig. 4: a) Pulse train and b) single pulse waveforms of the passively q-switched laser for 5W of absorbed pump inside the Yb:KGW crystal.*

Fig. 4 illustrates the temporal trace of q-switched regime for a 5 W absorbed pumping in the laser crystal. Fig. 4.a shows the qswitch pulse train with a repetition frequency of 9 kHz. Fig. 4.b shows the waveform of the generated pulses with a width of 25 ns (FWHM) measured at the output of M4 and corresponds to a peak intracavity power of 50 kW.

### 3.3.- Resolution enhancement with asymmetric SFM pump

The shape and size of the intacavity laser mode (1040 nm, SFM pump) act as a soft-aperture in the Fourier plane of the upconverter, allowing the transmission (or conversion) of a larger or smaller number of spatial frequencies of the infrared illumination. The physical aperture represented by the CPLN crystal (1 mm (vertical) x 3 mm (horizontal)) imposes limitations, primarily in the vertical direction, on the maximum attainable mode size and, consequently, on the resolution. When taking into account the thermal lens in the Yb:KGW crystal (for 5 W absorbed at 981 nm) and when properly adjusting the cavity size, and the position of the ICL (Fig. 1), the laser mode can be oscillated with a diameter close to 2.5 mm at the CPLN crystal position.

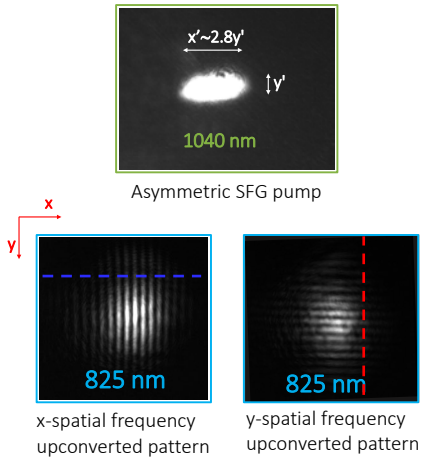


*Fig. 5: Asymmetric SFM pump profile and upconversion of x-oriented and y-oriented patterns.*

In this configuration, with the CPLN crystal inside the cavity, an aperture effect is observed in the vertical direction, resulting in an asymmetric laser mode where the horizontal width is approximately three times the vertical width. This configuration enables the enhancement of image resolution for spatial frequencies aligned with the widest axis of the pumping mode (y-axis). As illustrated in Fig. 5, the asymmetric intracavity laser mode at 1040 nm facilitates a higher resolution conversion for a given spatial frequency when oriented horizontally with respect to the vertical orientation. A mid-IR (4 µm) pattern with a single period of 0.4 mm, oriented in both *x* and *y* axes, is upconverted to 825 nm. The enhancement in resolution is clearly observable in the upconversion for the *x* axis orientation.

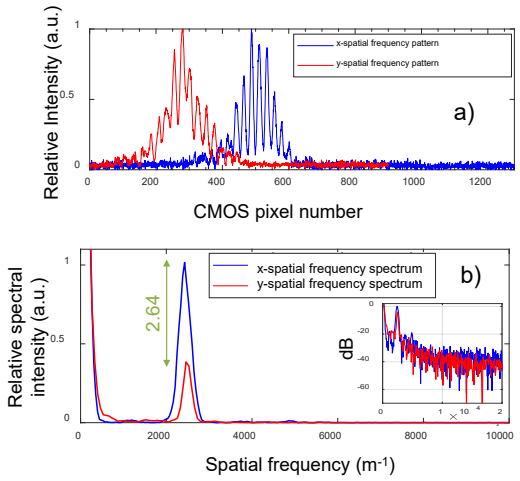


*Fig. 6: a) Lines of pixels and b) FFT spatial frequency spectrum of x-oriented and y-oriented patterns.*

The dashed lines (blue and red) represent a single line of pixels of the upconverted image in either horizontal (red) or vertical (blue) pattern orientation. These were extracted from image areas where their corresponding pixels were not saturated, and their information is analyzed in Fig. 6. Fig. 6 a) displays the normalized intensity versus pixel number of the analyzed line for both horizontal (blue) and vertical (red) orientation. It is evident from this figure that for the x-oriented pattern a better image contrast is obtained than for the y-orientation due to a smaller aperture effect in the x-orientation, where the SFM pumping mode is wider. From Fig. 6.a, in Fig. 6.b. we obtained, by FFT, the spectrum of spatial frequencies present in the converted image when the pattern is oriented in both x and y directions. In this representation (Fig. 6.b) the horizontal axis has been rescaled to represent the spatial frequency of the mid-IR image, instead of the NIR converted one, which is not the same due to the angular reduction of the conversion process. The figure illustrates the squared amplitude of the spatial frequencies of the 4 µm image pattern within the spatial frequency spectrum of the converted image upon orientation. The periodicity of this pattern is 0.4 mm, corresponding to a spatial frequency of 2500 $m^{-1}$. For this spatial frequency, the intensity of the pattern frequency in the spectrum for the x-orientation is 2.64 times higher than for the y-orientation, which roughly corresponds to x-axis and y-axis gaussian apertures with a ratio of widths 1/e of 2.8 (Fig. 5).

## 4.- Conclusion

This work demonstrates significant advancements in mid-IR imaging through the development of an Yb:KGW laser-based image upconverter. By integrating a CPLN crystal, broad SFM pump beams, and q-switched intracavity conversion, we have achieved enhanced spectral and angular acceptance, high spatial resolution, and improved conversion efficiency. The experimental results confirm the successful real-time upconversion of mid-IR images to NIR. The use of asymmetric laser modes within the cavity further enhances image resolution, particularly for spatial frequencies aligned with the widest axis of the pump mode. These improvements address the limitations of traditional mid-IR imaging systems, offering a high-performance solution that can be applied in various fields requiring advanced imaging capabilities. Future work will focus on optimizing these parameters further and exploring additional applications of this technology.

*Acknowledgements*: This work has received financial support from Agencia Estatal de Investigación (Grant PID2020-117658RBQ1

I00, MICIU/AEI/10.13039/501100011033); European Regional Development Fund; Conselleria de Innovación, Universidades, Ciencia y Sociedad Digital, Generalitat Valenciana (Grant CIAICO/2021/326).

*References*

[1] J. Dam, P. Tidemand-Lichtenberg, and C. Pedersen, "Room-temperature mid-infrared single-photon spectral imaging," Nature Photon 6, 788–793 (2012).

[2] A. Barh, P. J. Rodrigo, L. Meng, C. Pedersen, and P. Tidemand-Lichtenberg, "Parametric upconversion imaging and its applications," Adv. Opt. Photon. 11, 952-1019 (2019).

[3] C. Pedersen, E. Karamehmedović, J. Dam, and P. Tidemand-Lichtenberg, "Enhanced 2D-image upconversion using solid-state lasers," Opt. Express 17, 20885-20890 (2009).

[4] K. Huang, J. Fang, M. Yan, et al. "Wide-field mid-infrared single-photon upconversion imaging," Nat Commun 13, 1077 (2022).

[5] T. Zheng, Z. Wei, K. Huang, M. Yu, J. Fang, Z. Wen, J. Zhang, and H. Zeng, "Mid-infrared Fourier ptychographic upconversion imaging," Optica 11, 1716-1724 (2024).